2021 43rd Annual International Conference of the
IEEE Engineering in Medicine & Biology Society (EMBC)
Oct 31 - Nov 4, 2021. Virtual Conference

Estimating the Center of Rotation of Tomographic Imaging Systems with a Limited Number of Projections

Huanyi Zhou[†], Stanley J. Reeves[†] and Peter R. Panizzi[*]
[†]Electrical and Computer Engineering
[*]Drug Discovery and Development, Harrison School of Pharmacy
Auburn University, USA

ABSTRACT

For a tomographic imaging system, image reconstruction quality is dependent on the accurate determination of coordinates for the true center of rotation (COR). A significant COR offset error may introduce ringing, streaking, or other artifacts, while smaller error in determining COR may blur the reconstructed image. Well known COR correction techniques including image registration, center of mass calculation, or reconstruction evaluation work well under certain conditions. However, many of these methods do not consider various real-world cases such as a tilted sensor or non-parallel projections. Furthermore, a limited number of projections introduces stripe artifacts into the image reconstruction that interfere with many of these classic COR correction techniques. In this paper, we propose a revised variance-based algorithm to find the correct COR position automatically prior to tomographic reconstruction. The algorithm was tested on both simulated phantoms and acquired datasets, and our results show improved reconstruction accuracy.

Keywords — Tomographic imaging; COR correction; OSTU; Variance; Limited Projections

1. INTRODUCTION

Computed tomography (CT) reconstructions are based on the use of the inverse Radon transform, which assumes that the object is centered and stationary [1]. In some applications of tomography, the center of rotation (COR) is not predetermined. One such example is data collected from a X-ray imager equipped with a sample rotation system that turns the sample between acquisitions rather than having the source and sensor rotate on a gantry moving around the sample [2]. Because the sample in the spinning system may not be placed precisely or consistently relative to the imaging coordinate system, the COR is often uncertain. In addition, the sample may not consistently spin around an assumed axis because of variations in the attachment to the holder or due to gravity. Therefore, the specimen presented in the projection images may appear to be tilted or off center. As a result, the reconstruction of such datasets may show ringing or streaking artifacts [3]. Existing COR correction techniques can be divided into two categories, pre-calibration algorithms with a known phantom [4] and retrospective calibration algorithms with a specific cost function [5]. For an inserted spinning system where the scanning position varies each time due to manual placement, pre-calibration is not appropriate while retrospective calibration utilizing the projection image information directly has proven effective in solving such problems.

Previous research has explored the misalignment errors caused by different factors [6]. Results show that bias in the COR and the in-plane rotation cause the most serious distortion in reconstruction. Several methods have been proposed to calculate the displacement of the rotation center. Zhu *et al*. [7] and Li *et al.* [8] developed an automatic COR correction method by calculating the center-of-mass in parallel scanning mode and estimating the displacement by least squares. Yu *et al*. [9,10] extended the method to fan-beam scanning mode and added rotation error into consideration. However, it has been shown to be sensitive to light scattering, diffraction, and reflection effects [11,12]. Meng *et al*. [13] and Tilman *et al*. [14] utilized the feature that two opposing projection X-rays across the COR can give rise to the same projection data, known as the image registration method, to estimate the COR by finding the maximum correlation coefficient point along projections. Nghia *et al*. [12] proposed a quality assessment algorithm based on the observation that significant Fourier transform coefficients of the sinogram image appear in a certain region in the frequency domain [15].

However, our investigation has observed that this algorithm is sensitive to the filtering function that must be set manually and the number of projection images. An improved metric estimation strategy in COR determination was proposed by Dong *et al*. [11,16] based on the variance estimation method [17]. Our work confirms this method and its superior performance in phantom simulation but only when given ample projections. However, in practice, its accuracy degrades in the low signal-to-noise (SNR) ratio case under a limited number of projections.

Our method overcomes the limitations of the variance estimation method by introducing a modified variance-based algorithm. First, we propose a new coarse search strategy prior to the variance-based search. This limits the search space required by the more computationally intensive variance-based search. We use an edge detection algorithm on the cylinder containing the scanned object to align the depth axis of the projection image instead of employing the centroid method. This approach avoids problems with low-contrast images. We derive the geometric relations between the image edge locations and the three-dimensional tilt and shift parameters of the object that are used to initialize the variance-based search. Due to space considerations, our derivations are documented separately [18]. Second, our algorithm distinguishes the object from the background noise to calculate a normalized variance. This strategy is based on the observation that severe artifacts often appear outside the region of support (ROS) merely due to the limited number of projections. A small COR error that introduces blur can actually mitigate the artifacts outside the ROS, leading to a misleading quality metric when using a global criterion.

2. INSTRUMENT AND METHODS

2.1. Instrument

Our studies used an In Vivo Imaging System (IVIS) Lumina XRMS machine equipped with MiSpinner [2], to acquire X-ray projection images and rotate the sample between acquisitions. The main imaging chamber of the IVIS system consists of a fixed-position X-ray source at the bottom, a scintillation plate, and an overhead CCD camera. The scintillation screen is used to convert the X-rays into photons of light that can be collected by the super-cooled camera. X-ray projection images can be acquired at different contrast levels under the fixed 10×10 cm^2 field of vision. The MiSpinner itself consists of a 50-mL conical mouse holder and an actuated motor on a 3D printed stage. An actuator motor rotates the mouse holder to form an iso-center projection image stack.

2.2. Coarse Search

A coarse-fine search strategy was first proposed in [11] for automatic COR position determination in an optical system. In the coarse search, they applied the center-of-mass algorithm to estimate the raw COR position given the assumption that the system works in parallel projection mode. However, in small animal research, this assumption is not satisfied.

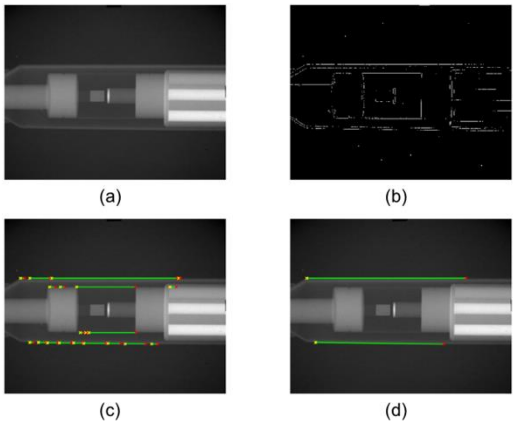

Fig. 1. Coarse search in CT phantom raw COR determination. (a) One projection image of CT phantom, (b) Binary image after Canny filtering, (c) Edge detection after Hough Transform, (d) Edge determined after RANSAC selection.

Instead, a coarse estimation of COR can be simply realized by calculating the average of two edges. The edges of the holder tube can be used as an indicator of the upper and lower boundaries, which are approximately equally displaced from the nominal axis of rotation.

$$\mathrm{COR}_{\mathrm{raw}} \approx \frac{\mathrm{P}_{\mathrm{upboundary}} + \mathrm{P}_{\mathrm{botboundary}}}{2}$$

The boundaries of the holder have low contrast in the projection images. To address this problem in edge determination as Fig. 1(b) shows, we combine the Hough Transform and RANSAC selection technique as Fig. 1(c-d) shows. An average calculation on 0, 90, 180 and 360 projection images are taken to further remove the error caused by light scattering or device vibration during measurement. After the rotation axis position is determined, in-plane rotation degree η is estimated by calculating the angle between the rotation axis and the lateral axis according to [18].

Three main advantages of the proposed coarse search step are as follows: 1) easy to realize and robust; 2) independent of the scanning mode; and 3) applicable to in-plane rotated projection images.

2.3. Fine Search

Once the center of the holder is determined, the fine search region is set to +/- 30 pixels. Then we evaluate the reconstruction image quality by metric evaluation algorithm for each possible COR position. In [11], the evaluation is defined on the global variance of the reconstruction image, based on the assumption that the maximum variance occurs when reconstructing with the correct COR [3]. Unfortunately, this does not hold for the low dose case where global variance estimation is highly affected by the presence of scattering and blurring as well as the extra background structure caused by a limited number of projections. Therefore, we use a multilevel thresholding on the image histogram with Otsu's method to distinguish the ROS from the background under two assumptions: 1. background artifact values are generally smaller than specimen values, and 2. most variance contributions are from high-value components. A revised variance estimation metric can be described as:

$$Q_{var} = \frac{\sum\sum\left(\tilde{I}(x,y) - \bar{\tilde{I}}\right)^2}{\tilde{N}^2}$$

where

$$\tilde{I} = Otsu(I,n) * I$$

$$\text{Otsu}(I,n) = \arg\max\{(\sigma_B')^2\{t_1, t_2, \dots, t_{n-1}\}\}$$

$$(\sigma_B')^2 = \sum_{k=1}^{n} \omega_k \mu_k^2$$

I is the reconstruction result, $\tilde{I}$ is the reconstruction after multilevel thresholding, $(\sigma_B')^2$ is modified between-class variance and $t_1, t_2, \dots, t_{n-1}$ are multilevel thresholds in the histogram. Multi-level thresholding can be used to focus the variance calculation on image contents rather than background areas with noise.

For each reconstruction in the fine search range, the maximum value of Q_{var} indicates the correct COR position, and its corresponding position in the fine search region can help locate the correct COR.

3. EXPERIMENTS

3.1 Phantom Simulation

To validate the usefulness in the case of a limited number of projections, both variance-based and modified criteria were tested on the Shepp-Logan phantom in an interval +/- 15 pixels away from the correct COR position with various numbers of projections. As Fig.2 shows, an evaluation curve was obtained after an exhaustive estimation on 31 reconstruction images. Both algorithms found the correct COR position corresponding to the largest value in its estimation curve. Our proposed criterion can produce similar performance compared with the widely used global variance estimation algorithm in high contrast situations.

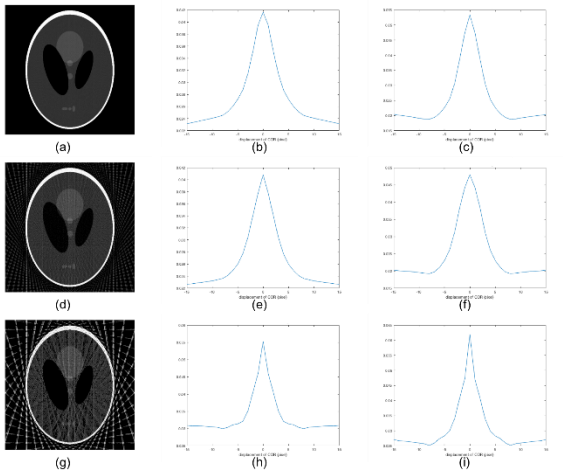

Fig. 2. Fine search test on Shepp-Logan phantom with various numbers of projections. (a), (d), (g) are correct reconstruction images from 360, 97 and 40 projections. (b), (e), (h) are estimation results from variance-based algorithm in paper [11], (c), (f), (i) are results from our method. X-axis is the search range from -15 to 15 pixels.

3.2. Mouse Data Test

Besides the phantom data simulation, coarse-fine search was also applied on actual data to test its feasibility. In our research, both criteria were tested on a mouse dataset obtained from the IVIS imaging system with 97 projections in a full scan. For this study, a total of 4 C57BL/6 mice were produced by an in-house breeding colony maintained under protocol number 2018-3438, as approved by the Institutional Animal Care and Use Committee of Auburn University. In this study, no living mice were imaged. The imaged carcasses were obtained from normal maintenance of a breeding colony. All mice were euthanized with CO2 asphyxiation in accordance with the Guide for the Care and Use of Laboratory Animals of the National Institutes of Health. Each image size was 1024×1024 pixels. In order to compare their performance, the same coarse search was conducted first to make sure they exhaustively searched the same region. The raw FBP reconstruction result shown in Fig.3(a) has significant artifacts. Meanwhile, a rough estimate of the center of the tube by a coarse search is pixel coordinate 551, which becomes the center point for the fine search. Fig.3(c) describes the global

variance estimated by the normalized variance equation, and Fig.3(d) is local variance estimation after thresholding to eliminate the effect from the background. The COR with the highest score estimates the correct result and its position mapping to the desired COR position.

In Fig.3(c), the maximum value occurred at -1, indicating the axis equals 550. In Fig.3(d), the value occurred at -5, indicating a value of 546. Fig.3(e) and Fig.3(f) are corresponding reconstruction slices.

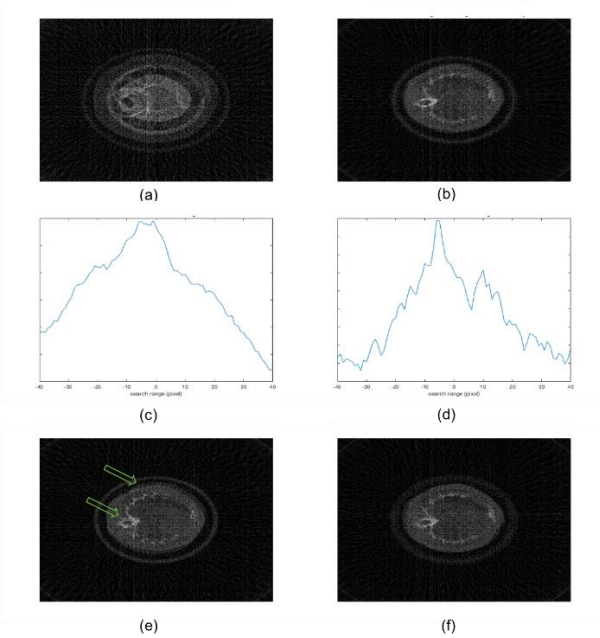

Fig.3. Application of coarse-fine search strategy on mouse dataset. (a) is FBP result of mouse data without any COR correction, (b) is the best reconstruction result found in the search interval, (c) is the normalized variance estimation curve in the interval, (d) is the curve from the modified method, (e) is the reconstruction result at the maximum point of the (c) curve, mis-aligned structures are pointed out by green arrows, (f) is the reconstruction result at the maximum point of the (d) curve, mis-aligned structure are fixed.

4. DISCUSSION

Structure mismatch can occur in both bone structure and soft tissue regions when COR errors are made, as seen in Fig.3(e). Besides, in low SNR cases, blur can act as a smoothing of the original signal that actually decreases the variance estimation when approaching the correct COR position. This can be observed as the flat region in the interval [-6,0] in Fig.3(c), where the correct COR position is obscured. Multilevel thresholding can successfully address this drawback by separating the ROS from the background to increase the usefulness of variance estimation at lower SNR and provide a clear and accurate maximum for COR position estimation.

In summary, our revised method shows superior performance on COR estimation given a limited number of projections in the case of low SNR.

REFERENCES

[1] Gabor T. Herman, " Image Reconstruction from Projections, the fundamentals of computerized tomography," 1980

[2] Andrew Brannen, M. E. & Panizzi, P. Correlation of 360-degree surface mapping in vivo bioluminescence with multispectral optoacoustic tomography in human xenograft tumor models. Sci. Reports 8, 3321, (2018).

[3] J. R. Walls, J. G. Sled, J. Sharpe, and R. M. Henkelman, "Correction of artefacts in optical projection tomography," Phys. Med. Biol., vol. 50, no. 19, pp. 4645–4665, 2005.

[4] Yang H, Kang K, Xing Y. Geometry calibration method for a cone-beam CT system. Med Phys. 2017 May;44(5):1692-1706. doi: 10.1002/mp.12163. Epub 2017 Apr 17

[5] Meng Y, Gong H, Yang X. Online geometric calibration of cone-beam computed tomography for arbitrary imaging objects. IEEE Trans Med Imaging. 2013 Feb;32(2):278-88.

[6] D. Xi *et al*., "The Study of Reconstruction Image Quality Resulting from Geometric Error in Micro-CT System," *2010 4th International Conference on Bioinformatics and Biomedical Engineering*, Chengdu, China, 2010, pp. 1-4

[7] Zhu et al., "Automated Motion Correction for In Vivo Optical Projection Tomography," in IEEE Transactions on Medical Imaging, vol. 31, no. 7, pp. 1358-1371, July 2012

[8] LI ZY, LÜ DH. " Fast-correction of rotating center offset with part views sinogram in 2D CT," CT Theory and Applications, vol. 24, no. 4, pp. 533-543. 2015

[9] Hengyong Yu, "Data Consistency Based Translational Motion Artifact Reduction in Fan-beam CT," IEEE Transactions on Medical Imaging, Vol. 25, No. 6, June, 2006

[10] Hengyong Yu, Ge Wang, "Data Consistency Based Rigid Motion Artifact Reduction in Fan-Beam CT," IEEE Transaction on Medical Imaging, Vol. 26, No. 2, Feb, 2007

[11] Dong D, Zhu S, Qin C. "Automated recovery of the center of rotation in optical projection tomography in the presence of scattering." IEEE J Biomed Health Inform. 2013 Jan;17(1):198-204.

[12] Nghia T.Vo, Reliable Method for calculating the center of rotation in parallel-beam tomography, Opt. Express, vol. 22, no. 16, 19078-19086(2014)

[13] Fanyong Meng, Zhongchuan Li, Accurate determination of the center of rotation for computed tomography, Chinese Journal of stereology and image analysis, Dec. 2013, vol. 18, No.4.

[14] Tilman Donath, Automated determination of the center of rotation in tomography data, J. Opt. Soc. Am. A, May 2006, vol. 23, No. 5.

[15] P. R. Edholm, R. M. Lewitt,, "Novel properties of the Fourier decomposition of the sinogram," Proc. SPIE 671, 8–18 (1986).

[16] D. Dong et al., "Analysis of the rotational center location method in Optical Projection Tomography," 2013 35th Annual International Conference of the IEEE Engineering in Medicine and Biology Society (EMBC), Osaka, 2013, pp. 3008-3011.

[17] Yu Sun, Stefan D, "Autofocusing in computer microscopy: Selecting the optimal focus algorithm," Microscopy Research and Technique, vol. 65, no. 3, pp. 139-149, 2004

[18] Huanyi Zhou, Stanley Reeves, Peter Panizzi, "Estimating the Center of Rotation of Tomographic Imaging Systems with Limited Projections – Detailed Explanation", Auburn University AUrora, http://dx.doi.org/10.35099/aurora-57